ACS Biomaterials SCIENCE & ENGINEERING
Cite This: ACS Biomater. Sci. Eng. XXXX, XXX, XXX−XXX
Article
pubs.acs.org/journal/abseba

Secretome-Based Prediction of Three-Dimensional Hepatic Microtissue Physiological Relevance

Amish Asthana,[†] Charles McRae White,[†] Kenneth Ndyabawe, Megan Douglass, and William S. Kisaalita*

Cellular Bioengineering Laboratory, College of Engineering, Driftmier Engineering Center, The University of Georgia, 597 D. W. Brooks Drive, Athens, Georgia 30602, United States

Supporting Information

ABSTRACT: Early biomarkers for indication of the complex physiological relevance (CPR) of a three-dimensional (3D) tissue model are needed. CPR is detected late in culture and requires different analytical techniques. Albumin production, CYP3A4 expression, and formation of bile canaliculi structures are commonly used to compare in vitro hepatic cells to their in vivo counterpart. A universal biomarker independent of the cell type would bring this to a common detection platform. We make the case that these hepatic characteristics are not sufficient to differentiate traditional (2D) cell culture from the more complex 3D culture. We explored the cytokine secretion profile (secretome) for its potential as a 3D early culture biomarker. PDGF-AB/BB and vascular endothelial growth factor (VEGF) were found to be upregulated in 3D compared to 2D cultures at early time points (days 3 and 4). These observations provide a foundation upon which in vivo validation of cytokines can lead to physiologically relevant 3D in vitro cell culture.

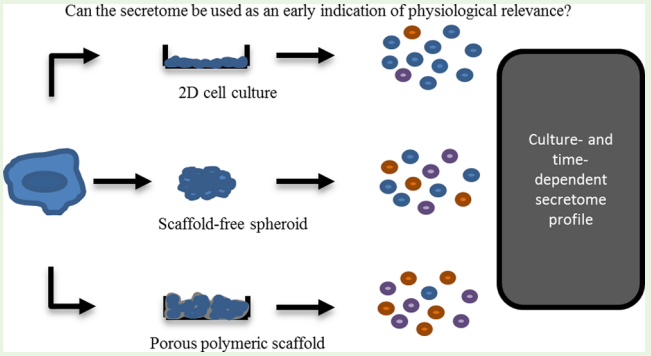

KEYWORDS: *cell-based assay, hepatic, scaffold, 3D culture, secretome*

1. INTRODUCTION

The inadequate predictive value of preclinical studies has resulted in the failure of more than 90% of compounds entering clinical trials, mainly due to insufficient efficacy and/or unacceptable toxicity,[1] resulting in higher drug-discovery costs. The use of three-dimensional (3D) microtissue-based drug discovery and therapeutics has the potential to increase the effectiveness of the discovery process, thus reducing the percentage of failures of compounds entering clinical trials. Despite their immense potential, access to 3D cell products and therapies is currently limited to leading clinical and research centers. At present, they can only be processed at small scales and at a high cost due to the lack of scale up in manufacturing technologies. Manufacturing 3D microtissues as a therapeutic product or an assay platform poses complex challenges, as very little standardization exists across the field for tissue characterization, physiological and phenotype markers, and functionality assays. The problem with the many emerging 3D platforms is that whenever 2D/3D culture differences are observed, "more physiological relevance" is claimed with no "gold standard" to substantiate the claims. Apart from the concept of "3D matrix adhesions" originally proposed by Cukierman et al.[2] as a possible indication or marker for a culture state of three-dimensionality, the field of tissue engineering has not provided knowledge on the basis of which a consensus for three-dimensionality and the associated "complex" physiological relevance (CPR) could be established. In the absence of standardized markers, reproducible and low-cost production of a high-quality product on a large scale is difficult to achieve, and the promise of 3D microtissue-based discovery and therapy cannot be fulfilled.

Traditionally, the meaning of three-dimensionality in cell culture has been simply associated with providing a 3D spatial microenvironment. In our recent work, the meaning has been extended to providing the total microenvironment that supports the formation of microtissues that exhibit CPR or better emulation of the in vivo microtissue functionality, in a manner not possible in 2D cultures.[3] The literature has provided guidance that lead to four main categories or microenvironment factors (MEFs): (1) chemical or biochemical composition, (2) temporal and (3) spatial (geometric 3D) dimensions, and (4) biophysical or substrate physical properties.[3]

The main aim of the research being conducted in the field of 3D cell culture is to provide cells with an in vivo-like microenvironment so that their behavior is closest to that of the native tissue. Therefore, many novel 3D platforms in research exist (and a few that are commercially available) that

Received: September 21, 2019
Accepted: November 20, 2019
Published: November 20, 2019

DOI: 10.1021/acsbiomaterials.9b01446
ACS Biomater. Sci. Eng. XXXX, XXX, XXX−XXX

provide varying degrees and different compositions of the above-mentioned microenvironmental cues. To standardize 3D-based products and improve scalability, there is a need to establish which in vitro microenvironment (or platform) is optimum or supports the most in vivo-like culture. The major hindrance is that functional assays conducted on 3D tissues might not be the best way to assess which platform is the closest to in vivo. For example, hepatic cells grown on platforms, such as alginate hydrogel beads[4] and poly(L-lactic)acid (PLLA) microporous scaffolds,[5] that provide different microenvironmental compositions have yielded similar albumin secretion levels (all higher than 2D). It is possible that the difference in microenvironmental compositions in the two scenarios does not yield a significant effect on albumin secretion (i.e., functionality), and their inclusion in the platform design is redundant. It is also possible that the albumin assay is not adequately responsive in conveying the effect of the microenvironment on cellular function.[6] If the latter is true, then more functionality assays such as CYP450 activity, urea synthesis, and biliary excretion are needed to better understand the role differences in these two scenarios play in yielding the cell phenotype outcomes. Therefore, in general, a more complex secretion "signature" or "secretome", such as the cytokine secretion profile associated with this microtissue formation, should in principle be a better characterization of the microenvironment and serve as a yardstick for designing in vitro platforms.[7] The purpose of the work reported herein was to explore, as a first step, the potential of early cytokine secretion profiles in characterizing 3D platform microenvironments, with respect to supporting HepG2 cells exhibiting hepatocyte-like characteristics. We chose HepG2 human hepatocellular carcinoma cell line due to it being widely used as a liver toxicity model[8−10] as well as its well-characterized end-point structural physiological relevance—bile canaliculi formation.

2. MATERIALS AND METHODS

2.1. HepG2 Cell Culture. HepG2 human hepatocellular carcinoma cells (HB-8065) (ATCC, VA) were routinely cultured in 75 cm^2 tissue culture flasks in minimal essential medium containing 10% heat inactivated fetal bovine serum, 2.2 g/L sodium bicarbonate, 2 mM L-glutamine, and 1 mM sodium pyruvate in 5% CO_2 at 37 °C. At 75% confluence, the cells were detached by using Accutase and resuspended in the growth medium for plating.

2.2. Spheroid Fabrication. HepG2 spheroids (500, 1000, and 2000 cells/spheroid) were fabricated using the gravity enforced hanging drop method. Cells were counted using a Millipore Scepter 2.0 handheld automated cell counter. Cell solutions of 4000, 40 000, and 80 000 cells/mL in the growth medium were used to make 500, 1000, and 2000 cells/spheroid, respectively. Drops of cell solution (25 μL) were dispensed onto the underside of a 100 mm tissue culture plastic (TCP) dish lid using an 8-channel micropipette. Approximately 40 hanging drops were dispensed on each lid and then inverted and placed on the bottom half of the dish so that the drops hang off the lid. Approximately 3 mL of phosphate buffer solution (PBS) was dispensed in the bottom of each plate to prevent evaporation of the hanging drops. After 96 h of incubation, the spheroids were washed with growth medium and resuspended in dishes coated with 5 mg/mL poly(2-hydroxyethyl methacrylate) to avoid attachment.

2.3. Cell Number Determination and Spheroid Size Distribution. Using the PicoGreen dsDNA quantitation kit, double stranded DNA (dsDNA) was measured and used to determine cell number of 2D, spheroid, and scaffold samples. Briefly, spheroid samples were distributed to 1.5 mL Eppendorf tubes and washed with 1× TE solution (10 mM Tris-HCl, 1 mM EDTA, pH 7.5, no NaCl added) to dilute growth medium. The supernatant was carefully removed and discarded without disturbing the cell spheroids at the bottom of the tube, leaving behind 100 μL to ensure the spheroids are not removed from the tube. Spheroid samples were frozen at −80 °C for 24 h. After thawing, 100 μL of 2× cell lysis buffer was added to the spheroid samples in 100 μL of TE buffer to bring the total volume to 200 μL of 1× lysis buffer in TE. The spheroid samples were allowed to lyse for 30 min, vortexing briefly at the 15 min mark. For scaffolds with cells, each sample was washed with 1× TE buffer, aspirated, and frozen in −80 °C for 24 h. After thawing, 2 mL of 1× cell lysis buffer was added to each sample and allowed to incubate at room temperature for 30 min. The scaffolds and 2 mL of lysis buffer were then removed from MatTek plates, added to 15 mL Falcon tubes, vortexed briefly, and allowed the cells to lyse for another 30 min. The tubes containing spheroid and scaffold samples were centrifuged at 500*g* for 5 min to pellet cell and scaffold debris. Each sample (100 μL) was added to a 96-well plate, followed by 100 μL of the aqueous working solution of the Quant-iT PicoGreen reagent. The plate was allowed to incubate at room temperature for 5 min, protected from light. The samples were excited at 485 nm, and fluorescence intensity was measured at 520 nm using a Synergy HTX Microplate Reader.

2.4. Scaffold Fabrication and Culture. The microporous polymer scaffold was fabricated using the salt leaching method routinely used in our laboratory.[11,12] Briefly, polystyrene (PS) was dissolved in chloroform and then sieved sodium carbonate decahydrate particles were thoroughly mixed into the polymer solution. After chloroform was completely evaporated, the dishes were leached with water overnight. The average pore size of scaffolds A and B was found by the analysis of scanning electron microscopy (SEM) images to be (104 ± 4 μm, n = 13) and (175 ± 6 μm, n = 10), respectively. It was then treated with 0.2 M NaOH for 40 min at 40 °C, and after washing thrice with water, it was sterilized and coated with fibronectin (5 μg in 150 μL PBS). For seeding on scaffolds, cells were counted using a Millipore Scepter 2.0 handheld automated cell counter and 7 × 10^5 cells (in 140 μL medium) were added to each scaffold. After allowing 4 h for attachment, a fresh growth medium was added to bring the total volume to 1.5 mL in each plate. Half medium change was performed daily to ensure proper nutrient supply.

2.5. Scanning Electron Microscopy. Cell spheroids and cells on scaffolds were fixed with 2.5% glutaraldehyde in 0.1 M sodium cacodylate buffer, pH 7.2 for 1 h before rinsing in cacodylate buffer (without glutaraldehyde) three times, 15 min each. This was followed by postfixing with 1% OsO_4 in 0.1 M sodium cacodylate buffer for 1 h and rinsing in cacodylate buffer (without OsO_4) three times, 5 min each. The samples were then dehydrated successively in 30, 50, 70, 80, 95, and 100% ethanol for 10 min each. The scaffolds were then carefully removed from the dishes with an ultra-sharp blade and dried in a SAMDRI-780A critical point drier (Tousimis Research Corporation, Rockville, MD, USA). Spheroids and scaffolds were sputter-coated with gold for 60 s to achieve a coating thickness of about 15.3 nm. SEM images were captured with a FEI Inspect-F scanning electron microscope (SEM) (FEI Company, OR). A similar protocol was followed for scaffold samples without cells, with the exception that the preparation started with sputter coating.

2.6. Transmission Electron Microscopy. Cell spheroids and cells on scaffolds were fixed with 2.5% glutaraldehyde for 30 min and treated with 1% OsO_4 for 2 h at room temperature. Samples were subsequently dehydrated step-wise with ethanol (25, 50, 75, 95, and 100%) for 10 min followed by 100% propylene oxide (PO) twice for 20 min each. Upon dehydration, samples were then treated with 1:1 ratio mixture of PO and Embed812 resin overnight at room temperature. On the following day, the samples were placed into Embed812 resin for 30 min at room temperature before transferring into a 40 °C oven for another 30 min. The resin was subsequently changed followed by 1 h treatments at 45 °C and 1 h at 50 °C. Lastly, the samples were embedded with Embed812 resin at 60 °C for 24 h. Ultrathin sections of 70−90 nm thickness were sliced using a Reichert Ultracut S Ultramicrotome (Leica, Inc., Deerfield, IL), collected onto 200 mesh copper grids, and co-stained with uranyl acetate and lead

DOI: 10.1021/acsbiomaterials.9b01446
ACS Biomater. Sci. Eng. XXXX, XXX, XXX−XXX

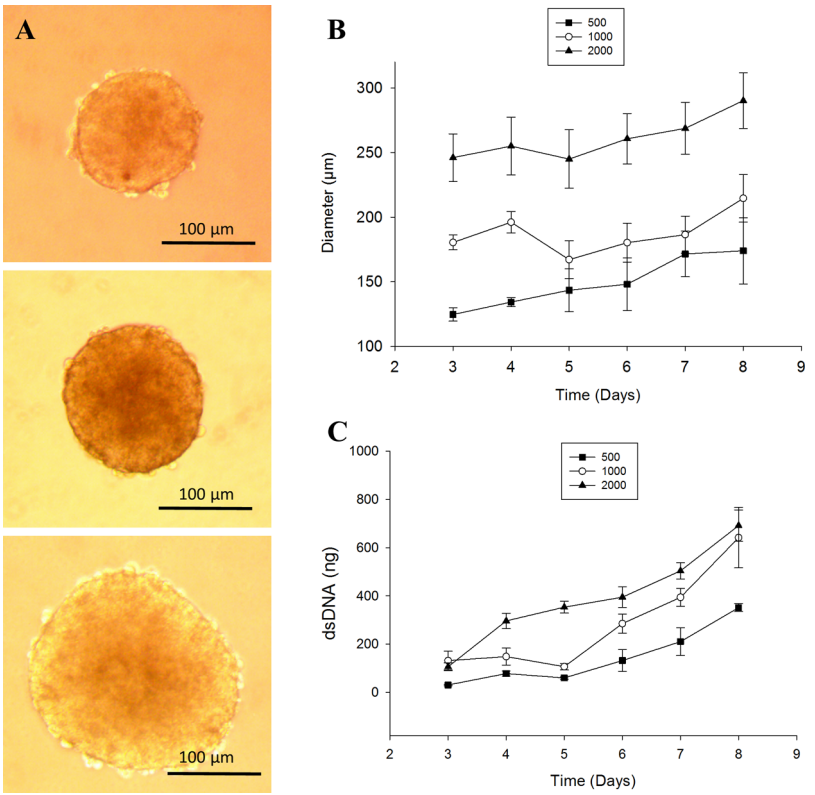

Figure 1. Growth profiles for HepG2 spheroids of various sizes. (A) Phase-contrast images taken on day 3 of 500, 1000, and 2000 cell HepG2 spheroid tissues grown using the hanging drop method. (B) Growth profile of 500, 1000, and 2000 cell HepG2 spheroid diameters after transferring from hanging drop to TCP dish, monitored using phase-contrast imaging and measured using ImageJ. (C) Growth profile of 500, 1000, and 2000 cell HepG2 spheroids after transferring from hanging drop to TCP dish, measured using Quant-iT PicoGreen dsDNA assay kit.

citrate for 10 min each. Observations were carried out with a transmission electron microscope (JEOL JEM-1011, Japan) at a voltage of 100 kV.

2.7. Hematoxylin and Eosin Staining. Fresh spheroids were embedded in OCT media, and 8 μm thick sections were cut using a Thermo Electron Corporation Cryotome. Subsequent washes were performed to remove excess OCT media and hydrate the sections. The nuclear detail was stained using Gill's II hematoxylin and a commercially prepared ammonium hydroxide solution was used to blue the hematoxylin. Water was removed from the sections using a series of ethanol rinses, followed by a commercially prepared eosin stain for the remaining tissue components. The sample was then treated with a solution (1:1) of xylene and acetone, followed by 100% xylene, which prepared it for cover slipping. A xylene compatible permanent mounting media was used to adhere the glass coverslip to the slide.

2.8. Albumin Secretion Assay. Albumin secretion from the different growth platforms was quantified by a sandwich enzyme-linked immunosorbent assay (ELISA) using a human albumin ELISA kit (Bethyl Laboratories, Montgomery, TX), according to manufacturer's protocol. Culture medium (200 μL) was collected every 24 h (for 8 days) and kept at −80 °C until analysis. The data were normalized against dsDNA at the respective time points, quantified using a PicoGreen dsDNA quantitation kit. One Way ANOVA was performed using a Student−Newman−Keuls method.

2.9. Cytochrome P450 3A4 (CYP3A4) Expression Assay. CYP3A4 activity was quantified using a Promega's P450-Glo bioluminescent kit (Madison, WI) that uses luciferin-IPA as the substrate. The manufacturer's protocol was followed. After 6 days of culture, to allow for attachment and development of a physiologically relevant tissue, the cells were induced with 50 μM dexamethasone. The medium was removed the subsequent day, and a new medium containing the same concentration of the inducer was added. After allowing for a total of 48 h of induction, the cells were washed, medium containing the substrate (luciferin-IPA) was added, and the cells were incubated for 60 min. After incubation, the cell culture supernatant was transferred to a white 96-well plate. The detection reagent supplied with the kit was added, and the bioluminescence was quantified using a Synergy HTX Microplate Reader. The cells were lysed and dsDNA was quantified using a PicoGreen dsDNA quantitation kit to normalize the CYP activity values with respect to the cell number. 2D cells were used for comparison. One Way ANOVA was performed using Student−Newman−Keuls method.

2.10. Cytokine Measurement and Principal Component Analysis. The Millipore (Burlington, MA) Milliplex MAP human high sensitivity cytokine/chemokine magnetic bead panel (measuring 21 analytes; EGF, GM-CSF, GRO, IFNg, IL-10, IL-13, IL1-B, IL-2, IL-6, IL-8, MCP-1, MDC, MIP-1a, MIP-1b, PDGF-AA, PDGF-AB/BB, RANTES, TGFa, TNFa, TNFb, and vascular endothelial growth factor (VEGF)) was used to analyze the cell culture supernatants from 2D, spheroids (500, 1000 and 2000 cells/spheroid) and scaffold (A and B) at the 24, 48, 72, and 96 h time points. These analytes were chosen because they have been shown to be upregulated in many different cell lines spanning various cell types. Manufacturer's instructions were followed. A minimum of 50 beads of each target analyte were acquired on a Luminex 200 instrument (Biorad). The concentration of each analyte in an unknown sample was estimated from a five parameter log−logistic calibration curve (5PL) fit to standards of known concentrations. Principal component analysis (PCA) was used to provide insights into the general differences of the secretome of different culture platforms. PCA converts possibly correlated variables, in this case cytokines, into linear combinations of the original variables that are uncorrelated with one another, termed principal components (PCs). Typically, only a few PCs maximally capture variability in the data set. The PCs can illustrate differences between the culture platforms. Computations were performed in SAS University Edition. Data points in scatter plots represent separate independent samples.

DOI: 10.1021/acsbiomaterials.9b01446
ACS Biomater. Sci. Eng. XXXX, XXX, XXX−XXX

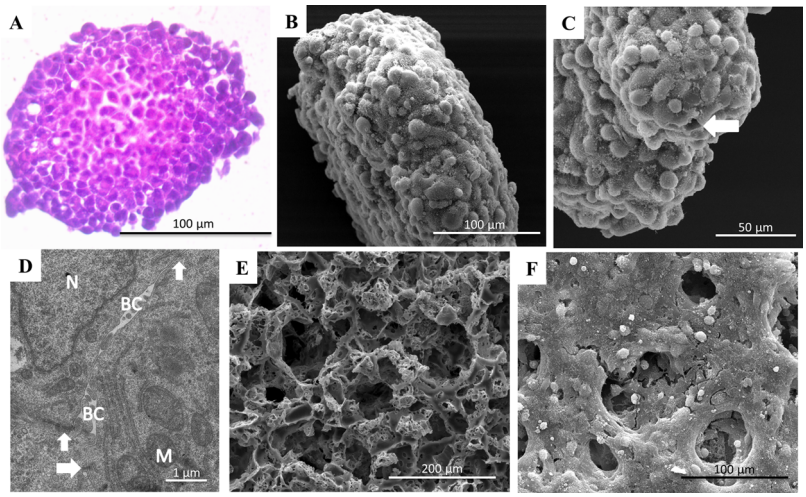

Figure 2. Qualitative investigation of HepG2 cell morphology and structural characterization using H&E (A), SEM (B,C,E,F), and TEM (D). (A) H&E staining on 1000 cell/spheroid on day 5 reveals cuboidal shaped cells in the center, more elongated cells on the surface, and the presence of bile canaliculi-like structures. (B) Further investigation of 1000 cell HepG2 spheroids reveals compact tissue formation and ECM deposition on day 5. (C) A small opening (white arrow) was observed on the outside surface, presumably an indication of bile canaliculi-like channel formation. (D) Structural characterization using TEM on scaffold A cultures on day 5 reveals microvilli-lined canaliculi and multiple cell to cell junctions. White solid arrow—tight junction, BC—bile canaliculi, M—mitochondria, N—nucleus. (E) SEM micrographs of NaOH/FN-treated 3D PS scaffold A (104 ± 4 μm, n = 13). (F) Homogenous tissue layer on the top surface while cells penetrate and close off the pores on day 3.

3. RESULTS

3.1. Characterization of HepG2 Cells from Different Platforms. The formation and progression of HepG2 cell spheroids were monitored every day using phase-contrast images for 8 days. Cells appeared as individuals or small aggregates within the hanging drop on days 1 and 2. Tissue-like spheroids of reproducible diameters for all the three cell numbers (500, 1000, and 2000 cells/spheroid) were fully formed by day 3 (Figure 1A), which resembled hepatocyte spheroids formed by various methods.[13,14] Once fully formed, the spheroid growth was monitored using phase-contrast imaging (Figure 1B). Spheroid proliferation was further assessed using a PicoGreen dsDNA quantitation kit and normalized to dsDNA, matching the growth trends observed by phase-contrast imaging (Figure 1C).

The viability and organization of HepG2 cells within the spheroids was studied on thin, hematoxylin and eosin (H&E)-stained cross-sections. H&E staining of spheroids on day 6 revealed cuboidal shaped cells in the center, while some cells on the surface had a more elongated shape (Figure 2A). Spheroids were fully formed after 3 days in the hanging drop format (Figure 1A). Transmission electron microscopy (TEM) and SEM were used to examine the ultra-structural features of HepG2 cultures. Individual cell boundaries on the spheroid surface on day 3 suggest that the cell aggregate is still in the process of forming a compact microtissue (image not shown). Fewer individual cell boundaries and the presence of fibrous ECM structures on day 5 indicate tissue formation (Figure 2B). SEM (Figure 2C) and TEM (Figure 2D) analyses of a 1000 cell spheroid on day 5 show the formation of bile canaliculi-like channels. These structures are lined with microvilli and distinguished by multiple tight junctions. The development of canaliculi-like structures was observed in all three spheroid sizes on day 5. SEM analysis of scaffolds showed similar structures between 1 and 2 μm in diameter by day 6, as reported in our previous publication.[12] The cells in spheroids (Figure 2D) and scaffolds[12] exhibited distinct nuclei and mitochondria, indicating cell viability.

HepG2 cultures grown on PS scaffold A (Figure 2E) and scaffold B (image not shown) were previously characterized in detail.[12] Briefly, cells formed compact tissues on the top surface and down into the scaffold pores by day 3 (Figure 2F). Tissue growth completely filled the pores in scaffold A (104 ± 4 μm, n = 13) by day 3 while most pores were filled in scaffold B (175 ± 6 μm, n = 10) by day 9.

3.2. Functional Physiological Relevance. 2D cultures produced more albumin than spheroid (500, 1000, and 2000 cell spheroids as a group) and scaffold (scaffolds A and B as a group) cultures on day 1 (Figure 3A). On days 2 and 3, both 2D cultures and spheroids produced more albumin than scaffold cultures. There was a continuous increase in scaffold culture albumin throughout the entirety of the experiment. Scaffold albumin surpassed 2D cultures by day 4 and spheroid cultures by day 6, reaching a maximum of 2.5 ng/ng dsDNA on day 8. The only differences among the different spheroid sizes were on day 1 where 500 cell spheroids produced less albumin than 1000 and 2000 cell spheroids and on day 7 where 2000 cell spheroids produced more albumin than 500 and 1000 cell spheroids. From day 3 onward, scaffold B albumin was significantly higher than scaffold A but less than 1-fold higher. Differences in albumin production between the three spheroid sizes and the two scaffolds can be found in Table S1. Although albumin production in spheroids increased during the first 5 days of the experiment, spheroids did not exhibit the same trend as their 3D scaffold counterpart during the last 3 days in culture. Rather, the albumin production decreased and was comparable to 2D cultures for the last 3 days. Therefore, we did not find albumin analysis adequate by itself to be a functional parameter for differentiating between 2D and spheroid culture conditions.

To perform a more comprehensive functional assessment of the platforms another hepatic function, cytochrome p450 (e.g., CYP3A4) expression, was used. CYP3A4 activity has been shown to be upregulated in alginate-encapsulated HepG2 (3D) but not in the 2D counterpart preparation.[15] Therefore, CYP3A4 activity might be useful as a marker for CPR.

DOI: 10.1021/acsbiomaterials.9b01446
ACS Biomater. Sci. Eng. XXXX, XXX, XXX−XXX

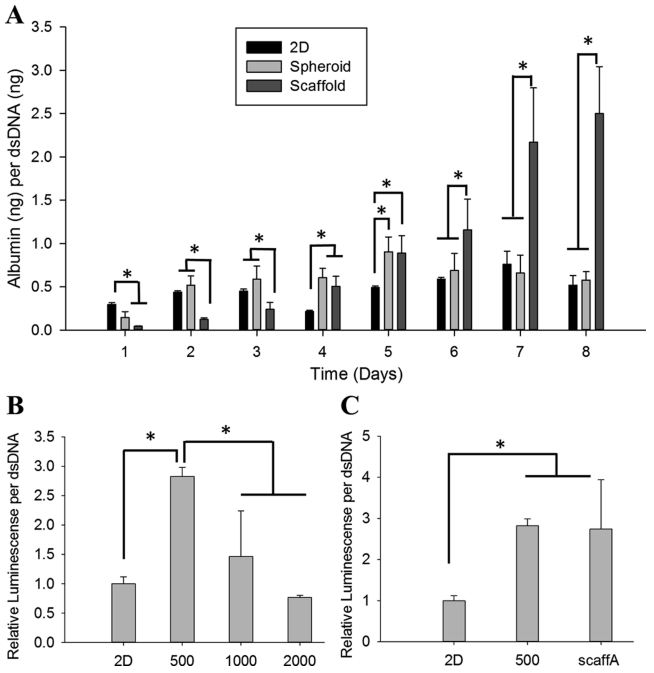

Figure 3. Assessment of functional physiological relevance using albumin production and cytochrome P450 (CYP3A4) activity. (A) 500, 1000, and 2000 cell spheroids are pooled together as "spheroid" and scaffolds A and B are pooled together as "scaffold". Albumin levels are low initially for scaffold cultures but become significantly higher than 2D on day 4 and significantly higher than spheroids on day 6. Albumin levels fluctuate over the 8 day experiment in 2D and spheroid cultures with no distinct trend. (B) CYP3A4 levels (presented as relative luminescence per dsDNA) is significantly higher in 500 cell spheroids compared with other spheroids and 2D, and similar to CYP3A4 levels in scaffolds (C) probably due to better diffusion of the substrate.

CYP3A4 activity in 500 cell spheroids was twice the activity observed in 1000 cell spheroids, and almost three times that observed in 2000 cell spheroids and 2D (Figure 3B). Scaffold A cultures had CYP3A4 activity comparable to 500 cell spheroids and significantly higher than 2D (Figure 3C). Therefore, CYP3A4 activity was able to differentiate between certain MEFs but not all platforms.

3.3. Cytokine Secretion Profile. Out of the 21 analytes used in the cytokine/chemokine panel, four cytokines (VEGF-A, IL-8, PDGF-AB/BB, and PDGF-AA) were chosen for further discussion as potential biomarkers as their production profiles showed maximum difference between 2D and 3D cultures. The remaining 17 analytes were either not expressed or not produced at a detectable level during the first 4 days of cell culture. Vascular endothelial growth factor (VEGF) expression over time was significantly higher in scaffold cultures than any other platform (Figure 4A). On day 1, The VEGF expression in scaffold cultures was 3.6-fold higher compared to 2D cultures and 1.8-fold higher compared to spheroids (Table 1). Over time, the VEGF production in scaffolds increased compared to spheroids and 2D, being 8.2-fold and 36.5-fold higher by day 4, respectively. There was no significant difference in VEGF expression between the two scaffold types. There was no difference in VEGF expression among the different spheroids, except for 500 cell spheroids not expressing VEGF on day 3. The production profile in 2D cultures for VEGF was similar to the profile of other analytes, reaching a maximum production on day 2 (0.17 μg/dsDNA) and then decreased on days 3 and 4.

2D cultures did not produce PDGF-AB/BB at any time point (Figure 4B). There was very little PDGF-AB/BB expression in the 3D cultures on day 1 (spheroid, scaffold). By day 2, both scaffold types had a significant increase, with scaffold B having 0.9-fold higher PDGF-AB/BB production compared to scaffold A (Table 1). A shift in expression was observed on day 3, with scaffold A 0.7-fold higher than scaffold B. By day 4, scaffolds A and B had comparable PDGF-AB/BB production. The trend over the first 4 days in culture for both scaffolds was similar to the production trend observed in VEGF. PDGF-AB/BB production increased during the first 3 days and reached a maximum in 2000 cell/spheroid cultures on day 3 (0.065 μg/dsDNA). 1000 cell/spheroid on day 4 was the only other time point spheroids expressed PDGF-AB/BB and had production comparable to 2000 cell/spheroid cultures. PDGF-AB/BB was only expressed in 500 cell/spheroid on day 4.

IL-8 expression in 2D cultures was significantly higher than both spheroid and scaffold cultures (Figure 4C). On day 2, IL-8 in 2D cultures was at its highest (0.63 μg/dsDNA), 4.3-fold higher than spheroid cultures and 23.4-fold higher than scaffold cultures (Table 1). IL-8 production decreased on days 3 and 4 in 2D cultures but was still 2-fold higher than both spheroid and scaffold cultures on day 4. The three spheroid sizes had similar trends, reaching a maximum production on day 2 (0.12 μg/dsDNA) but decreasing for days 3 and 4. IL-8 production in spheroids, however, was significantly lower compared with 2D cultures at all time points. Spheroids (as a group) initially produced more IL-8 compared to the scaffold cultures (A & B), but by day 4, the difference in production was no longer significant. There was no significant difference in IL-8 expression among the three spheroid sizes at any time point. Scaffolds expressed very low levels of IL-8 for all four time points, and there was no significant difference in the expression between the two scaffold types. Whereas 2D and spheroid cultures reached a maximum on day 2 followed by a decrease, IL-8 expression increased for both scaffolds A and B over the 4 days of culture, reaching a maximum on day 4 (0.0615 μg/dsDNA).

Trends similar to IL-8 production was observed for PDGF-AA for all platforms (Figure 4D). 2D cultures produced significantly higher levels of PDGF-AA on day 1 and reached a maximum production on day 2 (0.059 μg/dsDNA), 1.8-fold and 5.1-fold higher than spheroid and scaffold cultures, respectively (Table 1). PDGF-AA production in 2D cultures decreased on days 3 and 4 and was no longer significantly different than spheroid and scaffold cultures on day 4. Spheroids (as a group) reached a maximum production on day 2 (0.21 μg/dsDNA) and decreased on days 3 and 4. Spheroids initially produced more PDGF-AA, 1.8-fold higher on day 1 and 1.2-fold higher on day 2 but were not significantly different on days 3 and 4. There was no significant difference in PDGF-AA production among the three spheroid sizes at any time point. There was a continual increase in PDGF-AA production for both scaffolds A and B. By day 4, PDGF-AA levels in scaffolds were similar to 2D and spheroid cultures (0.016 μg/dsDNA). There was no significant difference in PDGF-AA production between the two scaffold types at any time point.

3.4. Principal Component Analysis. The secretome of all six culture platforms (in biological triplicates) were measured

DOI: 10.1021/acsbiomaterials.9b01446
ACS Biomater. Sci. Eng. XXXX, XXX, XXX−XXX

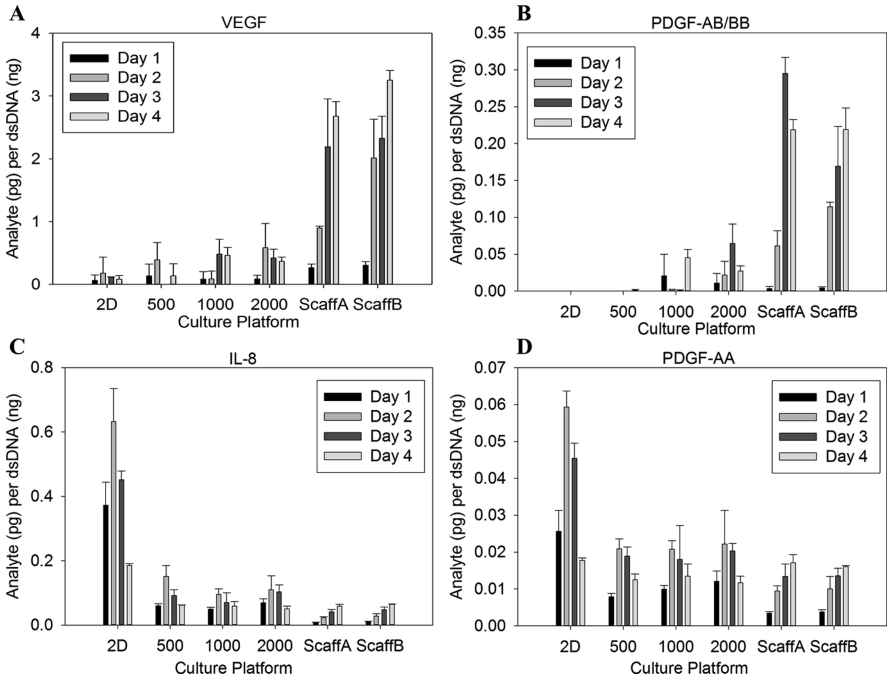

Figure 4. Production profile of four different cytokine analytes: VEGF (A), PDGF-AB/BB (B), IL-8 (C), and PDGF-AA (D). (A) VEGF levels increase each day for both scaffolds A and B cultures, while VEGF levels remain constant in 2D cultures. VEGF levels in the three different spheroid cultures on day 1 are comparable, but the individual profiles observed for the duration of the experiment do not share a common trend. (B) PDGF-AB/BB levels in scaffold B cultures increase in time similar to VEGF. Scaffold A cultures have higher PDGF-AB/BB levels on day 3 and comparable levels to scaffold B on day 4. 2000 cell spheroids were the only spheroid culture to produce PDGF-AB/BB for all time points. 1000 cell spheroids did not have detectable levels of PDGF-AB/BB on days 2 and 3. 500 cell spheroids only had detectable levels of PDGF-AB/BB on day 4. 2D cultures did not produce any PDGF-AB/BB. (C) Scaffolds A and B cultures had increasing IL-8 levels similar to the trends observed with VEGF and PDGF-AB/BB. IL-8 levels were the highest in 2D cultures, but after day 2, a decrease in IL-8 was observed. A similar trend was observed in all three spheroid cultures, where IL-8 levels reached a maximum on day 2 and decreased on days 3 and 4. (D) Scaffold cultures maintained the theme of increasing cytokine levels over time with PDGF-AA. 2D and the three spheroid cultures also had trends similar to those observed with IL-8. 2D and the three spheroid cultures reached maximum PDGF-AA levels on day 2, with a decrease in levels on days 3 and 4.

at the 24, 48, 72, and 96 h time points, giving a total of 72 observations. To gain an overview in how the secretome differs with respect to the culture platform and time, we used PCA. PCA yielded as many PCs as there were variables (4). By plotting the eigenvalues against the PCs and identifying the "elbow" of the curve, it was determined that the first two PCs explain a majority of the variation in the data (>95%). Therefore, we chose the first two PCs for analysis and interpretation of the data. Next, we identified the PCs that exhibit correlation greater than 0.5 (strong and positive) or less than −0.5 (strong and negative). IL-8 and PDGF-AB/BB were correlated with PC1 while VEGF and PDGF-AA were correlated with PC2.

The scatter plot of PC2 versus PC1 is shown in Figure 5. To make it easier to visualize, Figure 5 was broken into subplots by day (Figure S2A−D). Co-clustering of scaffolds A and B with the three spheroid sizes is evident on day 1, while 2D cultures are higher with respect to PC1 (Figures 5 and S2A). While scaffolds and spheroids remained co-clustered on day 2, 2D cultures remained separate and distinguished along PC1 and PC2 (Figures 5 and S2B). On day 3, scaffolds A and B appear to transition away from the three spheroid sizes with respect to PC1 and PC2 (Figures 5 and S2C). By day 4, scaffolds A and B are distinctively separate from 2D cultures and the three spheroid sizes with respect to PC1 and PC2 (Figures 5 and S2D). 2D cultures appear to be co-clustered with the three spheroid sizes on day 4 (Figures 5 and S2D). Co-clustering of the three spheroid sizes is evident for all 4 days.

PCA was also performed on the cytokine secretion profile combined with the albumin production for the first 4 days, to determine if the addition of a hepatocyte-specific function would change the clustering of the data. Adding albumin production to PCA did not change the trends or the PC correlations observed with cytokines alone (Figure S3). Taken together, early cytokine secretion profile, alone or in combination with albumin production, appeared to capture the time-dependent cellular response to the differences in its microenvironmental conditions.

4. DISCUSSION

Figure 1 demonstrates the constant spheroid proliferation rate from day 3 onward. The plateauing or slight decrease in proliferation between days 3 and 5 might be due to the transition of the spheroid samples from the hanging drop platform to a plate. Spheroids were transitioned from hanging drop as soon as they were fully formed to prevent potential nutrient limitations and enable easier medium change. During the first 2 days in the larger plate (days 3 and 4 of the experiment), individual cell boundaries on the surface of the spheroid became less defined while fibrous ECM became more abundant (termed "compaction"). On day 5, the spheroids resume their proliferative state. Similar spheroid formation time and high proliferation rates later in culture have been reported for the gravity-enforced hanging drop method.[14]

DOI: 10.1021/acsbiomaterials.9b01446
ACS Biomater. Sci. Eng. XXXX, XXX, XXX−XXX

Table 1. Cytokine Production Fold Change and Statistical Significance

	days in culture					days in culture			
VEGF	1	2	3	4	IL-8	1	2	3	4
2D/3D[a]	NS	NS	NS	-/16.4	2D/3D	8.4/-	6.7/-	5.4/-	2.1/-
2D/Sph	NS	NS	NS	NS	2D/Sph	5.2/-	4.3/-	4.1/-	2.3/-
2D/Scaff	-/3.6	-/7.1	-/18.8	-/36.5	2D/Scaff	40.8/-	23.4/-	9.1/-	2.0/-
Sph/Scaff[b]	-/1.8	-/3.1	-/6.5	-/8.2	Sph/Scaff	5.7/-	3.6/-	1.0/-	NS
500/1000[c]	NS	NS	NE/NA	NS	500/1000	NS	NS	NS	NS
1000/2000	NS	NS	NS	NS	1000/2000	NS	NS	NS	NS
500/2000	NS	NS	NE/NA	NS	500/2000	NS	NS	NS	NS
Scaff A/B	NS	NS	NS	-/0.2	Scaff A/B	NS	NS	NS	NS
	days in culture					days in culture			
PDGF-AA	1	2	3	4	PDGF-AB/BB	1	2	3	4
2D/3D	2.5/-	2.6/-	1.7/-	NS	2D/3D	NE/NA	NE/NA	NE/NA	NE/NA
2D/Sph	1.6/-	1.8/-	1.4/-	NS	2D/Sph	NE/NA	NE/NA	NE/NA	NE/NA
2D/Scaff	6.1/-	5.1/-	2.4/-	NS	2D/Scaff	NE/NA	NE/NA	NE/NA	NE/NA
Sph/Scaff[d]	1.8/-	1.2/-	NS	-/0.3	Sph/Scaff	NS	-/9.9	-/9.6	-/7.9
500/1000	NS	NS	NS	NS	500/1000	NE/NA	NE/NA	NE/NA	-/39.4
1000/2000	NS	NS	NS	NS	1000/2000	NS	NS	-/71.6	NS
500/2000	NS	NS	NS	NS	500/2000	NE/NA	NE/NA	NE/NA	-/23.2
Scaff A/B	NS	NS	NS	NS	Scaff A/B	NS	-/0.9	0.74/-	NS

[a]All spheroid and scaffold platforms are pooled together as "3D" and compared to 2D cultures to determine statistical significance using One Way ANOVA and Student−Newman−Keuls methods. For example, on day 1, the difference between 2D cultures and 3D cultures with respect to VEGF (pg) production per dsDNA (ng) was not significant (i.e., NS). [b]500, 1000, and 2000 cell spheroids are pooled together as "Sph" for spheroids. Scaffolds A and B are pooled together as "Scaff" for scaffolds. As another example, on day 1, the difference between spheroid cultures and scaffold cultures with respect to VEGF (pg) production per dsDNA (ng) was significantly different, with scaffold VEGF production 1.8-fold higher than spheroids. Scaffold cultures produced significantly more VEGF than spheroids cultures for all 4 days, with scaffold VEGF production 8.2-fold higher than spheroids on day 4. [c]500 cell spheroids did not express (i.e., NE) VEGF on day 3, making the comparison between 500 cell spheroids and 1000 cell spheroids not applicable (i.e., NA). [d]Spheroid cultures produced significantly more PDGF-AA (pg) per dsDNA (ng) when compared to scaffold cultures for the first 2 days. There was no statistical significance between the PDGF-AA production on day 3. On day 4, scaffolds produced significantly more PDGF-AA, being 0.3-fold higher than spheroids.

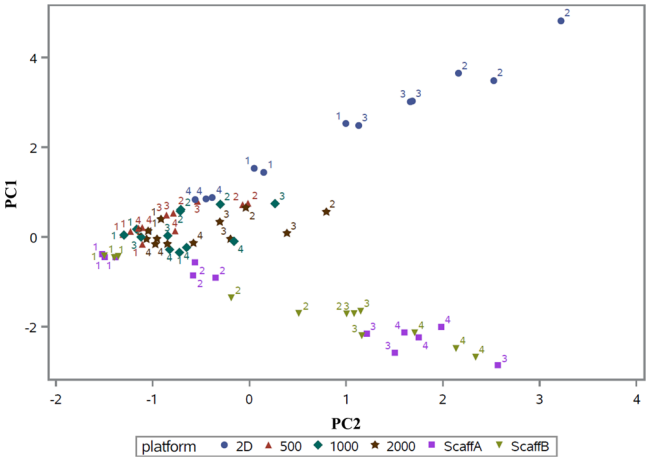

Figure 5. PCA of cytokine measurements for the top two PCs, which explained >95% of the results. Observations were color-coded by culture platform and represents an independent biological replicate. Each data point has been labeled with the day the sample was collected. Distinct co-clustering among the biological replicates of the same platform type (2D, spheroid, scaffold) on day 3 indicates this may be the best time to collect cytokines (also see Figure S2).

dsDNA levels in scaffold cultures started to plateau at day 3, while little to no cell proliferation was observed for the last 5 days in culture.[12] HepG2 cells grown on PS[16] and Matrigel[8] scaffolds have displayed a similar drop in the proliferation rate during the first 7 days in culture. Additionally, HepG2 cells grown on 2D TCP were highly proliferative throughout the experiment (Figure S1).

Consistent with other studies, providing a 3D geometric space for tissue formation promotes the adoption of a polarized phenotype in HepG2 cells. Hepatocyte polarity is a basic structural phenomenon in native liver tissues that is absent when cultured in 2D formats.[17,18] Polarization of hepatocytes in vitro has been correlated to many essential hepatic functions like biliary excretion, albumin secretion, and urea synthesis. Microvilli-lined bile canaliculi formation is also dependent on the polarized phenotype of hepatocytes. The polygonal network of bile canaliculi is formed by membranes contributed from the apical domain of contiguous cells, dividing the lateral domain of adjacent cells. Therefore, the presence of bile canaliculi-like structures can be used as a physical marker for CPR. As all the 3D tissue models (spheroid and scaffold) expressed the physical marker for CPR, it was not enough to determine the effect of each platform. Therefore, we decided to look at a functional aspect of the cells to determine which platform is emulating the in vivo microenvironment better.

Spheroid cultures showed high levels of albumin production during the first 5 days postseeding (Figure 3A). Interestingly, upon resuming a proliferative state on day 5, the cumulative albumin levels in the spheroid cultures decreased and maintained a consistently lower level of production. This relationship between HepG2 spheroid proliferation and albumin levels has been reported previously.[14] A similar relationship in cell proliferation and hepatocyte-specific function occurred in Matrigel-encapsulated HepG2 sphe-

DOI: 10.1021/acsbiomaterials.9b01446
ACS Biomater. Sci. Eng. XXXX, XXX, XXX−XXX

roids,[19] further supporting our results. Albumin production in our scaffold cultures was found to be significantly different from spheroids and 2D for all time points. Overall, scaffold cultures were not proliferating; however, albumin levels during this time steadily increased. This has been previously reported for HepG2 cells grown on PS[16] and Matrigel[8] scaffolds. Consistently low albumin production in 2D cultures indicate the same relationship between albumin production and cell proliferation that was observed in spheroid and scaffold cultures can be applied to 2D cultures. These results indicated that albumin production, a commonly used functional assay for analyzing the hepatocyte-like behavior of HepG2 cells, is not an adequate stand-alone functional parameter for differentiating between 2D and the more complex spheroid microenvironment.

The trends in CYP3A4 activity among the different spheroid models and the comparable activity in the 500 spheroids and the scaffolds might be due to diffusion of luciferin-IPA to the inner region of spheroids. Smaller spheroids have higher surface area to volume ratios compared to larger spheroids. Diffusion of luciferin-IPA to internal cells as well as the removal of metabolites is limited in spheroids with a larger diameter compared to smaller diameter spheroids and 2D cultures. A similar trend was observed in spheroids formed using inverted crystal colloid scaffolds.[13] At the time of induction (day 6), 500 cell spheroids were closest in size to the average pore size in scaffold A platforms, which might explain the comparable CYP3A4 activity on day 8. We speculate the difference in CYP3A4 activity is more reflective of the physical limitations in diffusion of the luciferin-IPA substrate than the cell function within the different microenvironmental conditions. Hence, structural (canaliculi) or functional (albumin/CYP3A4) cellular response, which is limited to a few assays, might not be adequate for comparing the effects of various microenvironmental factors. An additional molecular entity (cytokine secretion, in this case) that is independent of such limiting factors might be required for determining the conditions that promote hepatocyte-like behavior of HepG2 cells and establishing an optimal in vitro culture environment.

For us to determine whether cytokines can potentially be used as early markers for CPR, they should be able to distinguish between different environmental conditions. Regier et al. recently demonstrated that different pairings of cell lines and material composition influence the cytokine secretion profile, which gave rise to two distinct levels of response across cell lines.[20] Of the three tissue models (2D, spheroid, and scaffold), we have a distinct spatial MEF difference in 2D versus 3D geometry (3D being both spheroid and scaffold). By presenting a rigid scaffold that limits the maximum size of tissue growth within the scaffold pores, we have created a difference in the spatial MEF cues within the two platforms that can loosely be defined as "3D". Furthermore, the rigid scaffold provides a distinct biophysical MEF compared to the scaffold-free spheroid. Finally, to promote cell adhesion, we treated our scaffolds with a biochemical signal (fibronectin), whereas the spheroids were formed due to the forces of gravity. All four cytokines can be used to distinguish between the different MEFs (Table 1).

In terms of overall cytokine secretion, scaffold cultures follow a common trend. Analyte production was low on day 1 for all four analytes but increased for each consecutive day in culture. Overall analyte production in spheroid cultures does not follow an obvious upward trend like scaffold cultures, but a few analyte-specific trends were observed (Figure 4A–D). Although both spheroids and scaffold cultures can be loosely defined as "3D" because of the geometric nature of the tissues, there seems to be other factors that are affecting cell behavior. One factor to consider is the Young's modulus of synthetic polymers is above the physiological range.[12] Intuitively, our scaffolds do not provide an in vivo-like microenvironment. However, just the opposite was observed as the scaffolds showed a higher albumin production and CYP activity than 2D and spheroids. This might be due to the fact the scaffold is 89% porous and the Young's modulus is considerably lower for porous substrates compared to the bulk state.[6,12] Another possible explanation comes from the "cell-on-cell" hypothesis,[21] where cell to cell contacts appear to play a more pivotal role than cell to platform contacts. When cells are seeded at a high density as in the case of our scaffold, the numerous cell–cell interactions might supersede the cell–substrate interactions, leading to the formation of a cohesive microtissue such that only the outermost layer can "sense" the polymer substrate. Additionally, the deposition of endogenous ECM, which happens as early as day 3 in 3D cultures (Figure 2B,F) can provide a pliable microenvironment for the cells irrespective of the modulus of the scaffold.

The other factor to consider is when seeding cells on scaffolds, the empty scaffolds were overloaded with cells to ensure complete coverage of the scaffold surface and promote the quick formation of compact tissue, which helps minimize the effect of losing cells during medium change. Filling the scaffold pores with cells limited cell proliferation due to the size constraint posed by the rigid PS.[12] If cells are neither dividing nor preparing to divide they can be said to be in a state of quiescence, allowing them to allocate their energy to perform their main cellular functions. The same states of quiescence cannot be claimed for spheroid cultures for two reasons. Once fully formed spheroids are transferred from hanging drops to a larger dish. Because there is no physical constraint on spheroid size, their proliferation is not controlled. Additionally, HepG2s are derived from a perpetual human cancer cell line and will proliferate well past the hypoxia threshold if size is not constrained. Taken together, the adverse effects commonly associated with the polymeric scaffold for tissue culture did not seem to affect our cultures. In fact, limiting proliferation of hepatocellular carcinoma tissues by providing rigid pores improved the hepatocyte-specific functions.

Another trend involves the two analytes (IL-8 and PDGF-AA) that are upregulated in 2D cultures compared to 3D cultures (spheroid and scaffold). IL-8 and PDGF-AA levels reached a maximum on day 2 postseeding followed by a decrease for both 2D cultures and each of the three spheroid cultures (Figure 4C,D). By day 4 postseeding, analyte levels in scaffold cultures are either comparable (IL-8) or slightly higher (PDGF-AA) than spheroid cultures (Table 1). IL-8 production was significantly higher in 2D cultures; however, previous studies have shown IL-8 is significantly upregulated in 3D cultures compared to 2D cultures.[22−25] It is important to keep in mind that in our case, we are trying to determine which analytes can potentially be used as early detectors of CPR, while other studies have analyzed cytokine levels, including IL-8, to better understand the angiogenic capabilities and metastatic potential of cancer cells grown in vitro. These studies typically collect and analyze samples at a single endpoint weeks postseeding to allow for cell cultures to form

DOI: 10.1021/acsbiomaterials.9b01446
ACS Biomater. Sci. Eng. XXXX, XXX, XXX−XXX

tumor-like tissues. 3D cell culture systems are dynamic in nature compared to 2D and can behave differently with time.[26] Therefore, it is not unlikely that IL-8 levels in our spheroid and scaffold cultures could reach expression levels comparable to previous studies if the experiment was extended beyond day 4 postseeding. Furthermore, none of these previous studies report the temporal expression of IL-8 in 2D cultures.

VEGF expression was significantly higher in scaffold cultures compared to both 2D and spheroids during the first 4 days of culture. However, there was no significant difference in VEGF production when comparing 2D and spheroid. We speculate that VEGF is upregulated as a response to the unique combination of MEFs only present in the scaffold cultures and can potentially be used as an early indicator of CPR. PDGF-AB/BB is unique in that it was not expressed in 2D cultures for the first 4 days and only expressed in 500 cell spheroids on day 4. We observed higher PDGF-AB/BB production in 1000 and 2000 cell spheroids, which might suggest that 500 cell spheroids are not complex enough to produce PDGF-AB/BB. These results suggest PDGF-AB/BB can be used to differentiate between different spatial cues, such as microtissue size and 2D versus 3D cultures. VEGF is a multifunctional cytokine essential for hepatic vascular development.[27] Past studies have shown its upregulation in stem cell-derived hepatocyte-like cells[28] and HepG2 cells,[25] when cultured in 3D compared to monolayer cultures. PDGF-BB also plays a crucial role in vascular growth and stability.[29] The upregulation of VEGF and PDGF-AB/BB in 3D cultures constitutes the preliminary finding in support of further validation studies for early CPR biomarker potential.

Now that these cytokines have been established as potential markers that can distinguish between different MEFs, can we determine the best time to collect cytokines? PCA allows a complex data set to be plotted in just two dimensions and provides an illustration of differences in observations (e.g., culture platforms and time). If time-dependent differences in the secretome exist, the data for each culture platform for each time point should be separately clustered and distinguished along one or both PCs. Co-clustering of scaffold A with scaffold B as well as co-clustering of the three spheroid sizes in addition to a distinct separation from 2D on day 3 (Figures 5 and S2C) indicate this might be the best time to collect cytokines. By collecting cytokines on day 3, we also allow time for spheroid cultures to develop into compact microtissues. The addition of albumin production, which could not differentiate between 2D and spheroid cultures on its own, did not appear to change the clustering of the data (Figure S3). Therefore, these results indicate that early cytokine secretion profiles, by themselves or combined with albumin, can be useful for characterizing culture platform MEFs.

5. CONCLUDING REMARKS AND FUTURE OUTLOOKS

Typical end-point structural characterization of HepG2 3D culture—formation of bile canaliculi—associated with culture CPR, held across different platforms, including spheroids with different starting cell numbers and plastic scaffolds of different pore sizes. However, end-point functional characterization of HepG2 culture—albumin secretion and/or CYP450 activity—also associated with complex culture physiological relevance, was not as consistent across the same platforms. The up- and/or down-regulation of cytokines, secreted early in HepG2 3D culture (e.g., less than 4 days), including PDGF-AB/BB and VEGF, were responsive to different microenvironmental factors responsible for distinguishing not only 3D from 2D cultures but also among different 3D platforms, suggesting a promise of secretome-based early prediction of the HepG2 culture CPR outcome. In vitro validation of secretome-based CPR prediction with primary hepatocytes is needed before the hypothesis is tested in other cell types. A "reference" secretome can be realized by implanting the cells in vivo in a rodent, which provides an optimal "total microenvironment". The effect of the environmental cues can then be quantified in terms of the secretome, and an optimal environment can be engineered based on the secretome closest to the in vivo reference. This moves the assessment of the microenvironment away from end-point functional assays. As stated earlier, an assay chosen by an end user may or may not be responsive to the microenvironment. Once the in vivo secretome is established, the microenvironment can be deconstructed and the effect of each factor (i.e. spatial—size of the microtissue; biophysical—pliability (hydrogel type), rigidity (synthetic polymer scaffold), or scaffold free (spheroid); and biochemical—in vitro ECM/coating protein composition (adsorbed on surface or soluble in medium)) can be quantified, to be finally used to establish the optimal combination to reconstruct the ideal in vitro platform, using a "bottom-up" approach.

■ ASSOCIATED CONTENT

Supporting Information

The Supporting Information is available free of charge at https://pubs.acs.org/doi/10.1021/acsbiomaterials.9b01446.

Experimental details including additional experimental results (PDF)

■ AUTHOR INFORMATION

Corresponding Author

*E-mail: williamk@engr.uga.edu. Phone: (706) 542-0835. Fax: (706) 542-0886.

ORCID

William S. Kisaalita: 0000-0001-6999-8276

Author Contributions

†A.A. and C.M.W. contributed equally to this work.

Notes

The authors declare no competing financial interest.

■ ACKNOWLEDGMENTS

We thank Bobby Leitmann, Mary Ard, and Dr. John Shields for technical assistance.

■ ABBREVIATIONS

2D, two-dimensional; 3D, three-dimensional; CPR, complex physiological relevance; MEF, microenvironmental factor; TCP, tissue culture plastic; dsDNA, double stranded DNA; PS, polystyrene; PLLA, poly(L-lactic)acid; ECM, extracellular matrix; SEM, scanning electron microscopy; TEM, transmission electron microscopy; H&E, hematoxylin and eosin stain; VEGF, vascular endothelial growth factor; IL-8, interleukin-8; PDGF, platelet-derived growth factor; PCA, principal component analysis; PCs, principal components

■ REFERENCES

(1) Plenge, R. M.; Scolnick, E. M.; Altshuler, D. Validating therapeutic targets through human genetics. *Nat. Rev. Drug Discovery* **2013**, *12*, 581−594.

DOI: 10.1021/acsbiomaterials.9b01446
ACS Biomater. Sci. Eng. XXXX, XXX, XXX−XXX

(2) Cukierman, E.; Pankov, R.; Stevens, D. R.; Yamada, K. M. Taking cell-matrix adhesions to the third dimension. *Science* **2001**, *294*, 1708−1712.
(3) Lai, Y.; Asthana, A.; Kisaalita, W. S. Biomarkers for simplifying HTS 3D cell culture platforms for drug discovery: the case for cytokines. *Drug discovery today* **2011**, *16*, 293−297.
(4) Selden, C.; Shariat, A.; McCloskey, P.; Ryder, T.; Roberts, E.; Hodgson, H. Three-dimensional in Vitro Cell Culture Leads to a Marked Upregulation of Cell Function in Human Hepatocyte Cell Lines-an Important Tool for the Development of a Bioartificial Liver Machine. *Ann. N.Y. Acad. Sci.* **1999**, *875*, 353−363.
(5) Bierwolf, J.; Lutgehetmann, M.; Feng, K.; Erbes, J.; Deichmann, S.; Toronyi, E.; Stieglitz, C.; Nashan, B.; Ma, P. X.; Pollok, J. M. Primary rat hepatocyte culture on 3D nanofibrous polymer scaffolds for toxicology and pharmaceutical research. *Biotechnol. Bioeng.* **2011**, *108*, 141−150.
(6) Asthana, A.; Kisaalita, W. S. Biophysical microenvironment and 3D culture physiological relevance. *Drug Discovery Today* **2013**, *18*, 533−540.
(7) Asthana, A.; Kisaalita, W. S. Molecular basis for cytokine biomarkers of complex 3D microtissue physiology in vitro. *Drug discovery today* **2016**, *21*, 950−961.
(8) Luckert, C.; Schulz, C.; Lehmann, N.; Thomas, M.; Hofmann, U.; Hammad, S.; Hengstler, J. G.; Braeuning, A.; Lampen, A.; Hessel, S. Comparative analysis of 3D culture methods on human HepG2 cells. *Arch. Toxicol.* **2017**, *91*, 393−406.
(9) Ramirez, T.; Strigun, A.; Verlohner, A.; Huener, H.-A.; Peter, E.; Herold, M.; Bordag, N.; Mellert, W.; Walk, T.; Spitzer, M.; Jiang, X.; Sperber, S.; Hofmann, T.; Hartung, T.; Kamp, H.; van Ravenzwaay, B. Prediction of liver toxicity and mode of action using metabolomics in vitro in HepG2 cells. *Arch. Toxicol.* **2018**, *92*, 893−906.
(10) Yajima, Y.; Lee, C. N.; Yamada, M.; Utoh, R.; Seki, M. Development of a perfusable 3D liver cell cultivation system via bundling-up assembly of cell-laden microfibers. *J. Biosci. Bioeng.* **2018**, *126*, 111−118.
(11) Cheng, K.; Lai, Y.; Kisaalita, W. S. Three-dimensional polymer scaffolds for high throughput cell-based assay systems. *Biomaterials* **2008**, *29*, 2802−2812.
(12) Asthana, A.; White, C. M.; Douglass, M.; Kisaalita, W. S. Evaluation of cellular adhesion and organization in different microporous polymeric scaffolds. *Biotechnol. Prog.* **2018**, *34*, 505.
(13) Lee, J.; Cuddihy, M. J.; Cater, G. M.; Kotov, N. A. Engineering liver tissue spheroids with inverted colloidal crystal scaffolds. *Biomaterials* **2009**, *30*, 4687−4694.
(14) Mueller, D.; Koetemann, A.; Noor, F. Organotypic cultures of Hepg2 cells for in vitro toxicity studies. *J. Bioeng. Biomed. Sci.* **2011**, *S2*, 002.
(15) Lan, S.-F.; Safiejko-Mroczka, B.; Starly, B. Long-term cultivation of HepG2 liver cells encapsulated in alginate hydrogels: a study of cell viability, morphology and drug metabolism. *Toxicol. in Vitro* **2010**, *24*, 1314−1323.
(16) Bokhari, M.; Carnachan, R. J.; Cameron, N. R.; Przyborski, S. A. Culture of HepG2 liver cells on three dimensional polystyrene scaffolds enhances cell structure and function during toxicological challenge. *J. Anat.* **2007**, *211*, 567−576.
(17) Maurice, M.; Rogier, E.; Cassio, D.; Feldmann, G. Formation of plasma membrane domains in rat hepatocytes and hepatoma cell lines in culture. *J. Cell Sci.* **1988**, *90*, 79−92.
(18) Hubbard, A.; Barr, V.; Scott, L. Hepatocyte surface polarity. *Liver* **1994**, 189−213.
(19) Ramaiahgari, S. C.; den Braver, M. W.; Herpers, B.; Terpstra, V.; Commandeur, J. N.; van de Water, B.; Price, L. S. A 3D in vitro model of differentiated HepG2 cell spheroids with improved liver-like properties for repeated dose high-throughput toxicity studies. *Arch. Toxicol.* **2014**, *88*, 1083−1095.
(20) Regier, M. C.; Montanez-Sauri, S. I.; Schwartz, M. P.; Murphy, W. L.; Beebe, D. J.; Sung, K. E. The Influence of Biomaterials on Cytokine Production in 3D Cultures. *Biomacromolecules* **2017**, *18*, 709−718.
(21) Discher, D. E.; Janmey, P.; Wang, Y. L. Tissue cells feel and respond to the stiffness of their substrate. *Science* **2005**, *310*, 1139−1143.
(22) Fischbach, C.; Chen, R.; Matsumoto, T.; Schmelzle, T.; Brugge, J. S.; Polverini, P. J.; Mooney, D. J. Engineering tumors with 3D scaffolds. *Nat. Methods* **2007**, *4*, 855−860.
(23) Ghosh, S.; Spagnoli, G. C.; Martin, I.; Ploegert, S.; Demougin, P.; Heberer, M.; Reschner, A. Three-dimensional culture of melanoma cells profoundly affects gene expression profile: A high density oligonucleotide array study. *J. Cell. Physiol.* **2005**, *204*, 522−531.
(24) Fischbach, C.; Kong, H. J.; Hsiong, S. X.; Evangelista, M. B.; Yuen, W.; Mooney, D. J. Cancer cell angiogenic capability is regulated by 3D culture and integrin engagement. *Proc. Natl. Acad. Sci. U.S.A.* **2009**, *106*, 399−404.
(25) Leung, M.; Kievit, F. M.; Florczyk, S. J.; Veiseh, O.; Wu, J.; Park, J. O.; Zhang, M. Chitosan-alginate scaffold culture system for hepatocellular carcinoma increases malignancy and drug resistance. *Pharm. Res.* **2010**, *27*, 1939−1948.
(26) Asthana, A.; Kisaalita, W. S. Is time an extra dimension in 3D cell culture? *Drug discovery today* **2016**, *21*, 395−399.
(27) Carpenter, B.; Lin, Y.; Stoll, S.; Raffai, R. L.; McCuskey, R.; Wang, R. VEGF is crucial for the hepatic vascular development required for lipoprotein uptake. *Development* **2005**, *132*, 3293−3303.
(28) Leclerc, E.; Kimura, K.; Shinohara, M.; Danoy, M.; Le Gall, M.; Kido, T.; Miyajima, A.; Fujii, T.; Sakai, Y. Comparison of the transcriptomic profile of hepatic human induced pluripotent stem like cells cultured in plates and in a 3D microscale dynamic environment. *Genomics* **2017**, *109*, 16−26.
(29) Lange, S.; Heger, J.; Euler, G.; Wartenberg, M.; Piper, H. M.; Sauer, H. Platelet-derived growth factor BB stimulates vasculogenesis of embryonic stem cell-derived endothelial cells by calcium-mediated generation of reactive oxygen species. *Cardiovasc. Res.* **2009**, *81*, 159−168.

DOI: 10.1021/acsbiomaterials.9b01446
ACS Biomater. Sci. Eng. XXXX, XXX, XXX−XXX